ELSEVIER

Cement and Concrete Composites **19** (1997) 81–102

0958-9465/97/$17.00 + 0.00

PII:S0958-9465(96)00044-3

Deformation Measurements of Mortars at Early Ages and of Large Concrete Components on Site by Means of Embedded Fiber-optic Microstrain Sensors

W. R. Habel, D. Hofmann & B. Hillemeier*

Institut für Erhaltung und Modernisierung von Bauwerken e.V. (IEMB) Berlin (Institute for Rehabilitation and Maintenance of Structures), TU of Berlin, FB 9, Straße des 17. Juni 135, 10623 Berlin, Germany

Abstract

The paper demonstrates the application of fiber-optic microstrain gages to steel components of prestressed and reinforced concrete structures in order to measure deformations caused by proof loads or induced by constraints during the hardening period of large concrete sections. The use of embedded micro sensors for assessment of volume changes of cementitious building materials at early ages, and corresponding deformations due to heat, shrinkage, etc. in matured mortars, is also discussed. A resolution of 0.01 με was achieved. Theoretical aspects for the design of surface-mounted and embedded sensors are briefly addressed. We have investigated the behavior of embedded optical fibers, micro sensors and their coatings in cementitious mortars. Initial findings regarding the bond between sensor and the mortar matrix, as well as preferred coating materials, are presented. © 1997 Published by Elsevier Science Limited

Keywords: Optical-fiber sensors, structural element testing, embedment in concrete, damage assessment, mortar setting behavior.

INTRODUCTION

Optical-fiber sensors are predestined to monitor large structures and to measure strains over extended areas. Results have been published concerning sensor fibers which are based on intensity-modulated sensor arrangements or on the evaluation of the delay time characteristic of a transmitting fiber, and on the use of white light interferometry or similar effects.

Micro optic sensors—which enable deformations to be measured with very high resolutions and which are arranged either as simple sensors or as sensor chains (e.g. Bragg grating sensors)—are increasingly gaining recognition. The main advantages of miniaturized sensors are the following:

detection of very small reactions in the test object;
very high static and dynamic resolution of strain changes;
measuring signal not influenced by salts or water; and
possibility of obtaining absolute measurements even if the measuring equipment has been removed.

In order to obtain precise measurement data from the test object good contact between the sensor and the test object is necessary. This objective represents a considerable challenge for engineers, especially in civil engineering and more specifically in the field of concrete construction.

The present paper deals with the application of microstrain sensors (Fabry–Pérot type) in civil engineering structures, parts and materials. Based on the experiences gained from our applications we shall focus on some of the

*To whom correspondence should be addressed.

important problems that need to be considered and adequately solved in order to improve the capabilities of the present sensors. The key points of emphasis focus on the design of the microstrain sensors to arrive at a practicable arrangement for use on site, protection of the sensor and fiber components against mechanical and chemical attack, and achieving long-term stable operation. In addition, the paper includes a report on the results of volume change measurements on mortars during the hydration process at an early age by using a new design of stress-free microstrain sensor.

DEMANDS ON FIBER SENSORS TO BE APPLIED TO REAL STRUCTURES — OBJECTIVES

From the contractor's point of view

Although the capability of fiber-optic sensors has already been demonstrated in civil engineering applications, this new measurement technique has so far met with a hesitant response. The reasons may be the following:

high cost, including sensors, equipment and installations;

necessity to invest in new equipment (this is not the case for established measuring methods); and

difficulties in placement and/or embeddment of such sensors, and lack of knowledge thereupon.

For a wider acceptance of fiber-optic sensors the following points need to be considered:

a better price–performance ratio than with established sensors has to be achieved;

the method adopted for mounting the sensors and the installation of the sensor components must not hamper the construction process;

field equipment must be developed for a reliable use on site (no laboratory devices);

fiber sensors have to prove their efficiency in a direct comparison with established methods. (An application should be combined with alternative measurement techniques. The power line and the data recording equipment should be used separately in order to isolate special influences); and

for long-term measurement projects it must be possible for the service personnel to easily couple and decouple the sensors from the power line and the data recording equipment.

From the developer's point of view

In order to make use of the excellent features of fiber-optic microstrain sensors in civil engineering a number of very different problems has to be solved:

design of the sensor arrangement:

geometric dimensions of the active sensing area depending on the measuring requirements

design of a coating to suit the expected matrix

design of a sensor protective cover, if necessary;

knowledge of appropriate sensor materials for long-term stable operation under chemical and mechanical influences;

development of a reliable method of application in order to minimize subjective errors; and

development of a robust equipment capable of working on site under full climatic conditions.

The required R&D work can only be carried out by a suitably composed team of scientists, technicians and users.

DESCRIPTION OF THE FIBER SENSOR TECHNIQUE USED AND APPLICATIONS

The sensitive element described in this paper operates as an interferometric sensor (Fabry–Pérot type). It consists of a hollow glass tube about 15 mm long.[1] Into each side of the tube bare (uncoated) optical fibers are so inserted that their ends form a gap inside the tube. The end of the fibers are separated by a gap, s_o, and then fusion-spliced to the tube ends. For measurements of deformations the gap s_o is normally set at about 25 μm.

The sensor arrangement (Fig. 1) can be attached to the surface of a test object or embedded in a building material. A deformation of the test object produces a deformation of the tube, which in turn causes a variation of the gap between the movable fiber ends inside the tube. The measuring range is determined by the deformability of the hollow tube and by the distance of the fiber ends in their resting position. The resolution of this sensor arrangement is primarily determined by the wavelength of the laser source λ_S and the measuring instrument. A typical resolution for $\lambda_S = 1300$ nm is 0.06 $\mu\varepsilon$; at maximum it is 0.047 $\mu\varepsilon$. The sensi-

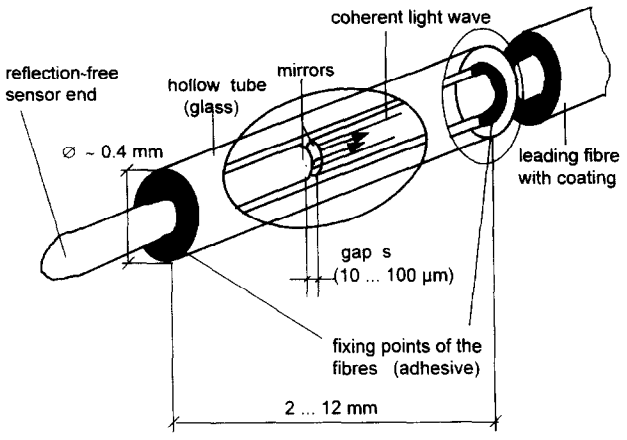

Fig. 1. Fabry–Pérot-type fiber-optic micro sensor.

tivity is significantly affected by the method of application.

The parameters of the micro sensor used are as follows.

Tube dimensions:
outer diameter: 250 μm
inner diameter: 128 μm
length: 12 mm.
Fibers inserted into the tube:
outer diameter (without coating): 125 μm
transmission (pigtail) fiber: single-mode
reflecting fiber: multi-mode.
Measuring basis: $\cong$10 mm (the measuring basis is reduced due to the fixing of the fibers onto the tube).
Measuring range (axial extension): $< +5000\ \mu\varepsilon$, $< -2500\ \mu\varepsilon$.
Vibration limit: 80 kHz (for axial extension: $< 10\ \mu$m).

The measurement principle is based on the superposition of coherent light waves reflecting in the two mirrors (= fiber end faces). Due to this superposition fringes are formed and at the output of the sensor (one fiber end of the sensitive element) the intensity I of interfering light can be recorded. This intensity I is a function of the gap s between the fiber ends:

$$I = I_0 \sin\left(\frac{4\pi sn}{\lambda_s} + \varphi_0\right) \tag{1}$$

where the temperature is constant, s is the distance between fiber end faces, n is the refractive index of the medium in the gap, λ_S is the wavelength of the source in vacuum, and φ_0 is the phase constant. The optical output signal corresponding to the actual spacing s of the mirrors is recorded by means of a photodiode. The axial strain changes of the complete sensor arrangement can be calculated from the intensity I using the relationship

$$\Delta\varepsilon = \frac{\Delta s}{L} \tag{2}$$

where L is the effective length of the sensitive element, typically dependent upon the length of the two fixed fiber ends. A transfer factor which depends on the method of application has to be taken into account, and has to be corroborated by test measurements. According to the measuring principle used, the sensitive element responds to an axial displacement of the fiber ends. However, because of the required difference in the diameters of the tube (inner diameter) and fibers, a small spacing between the fibers and the internal wall of the tube is formed. This can produce an angular misalignment of the parallel fiber end faces as a result of the splicing process used to attach the fibers on either end of the tube, or when a non-uniform lateral compression occurs along the tube.

From a theoretical estimation it follows that — in the worst case of an end face misalignment inside the tube — the measured strain value will be reduced by 0.2×10^{-6} of the strain value, i.e. for a maximum tube extension of 50 μm the value measured by the sensitive element is reduced by about 9 pm. This misalignment-induced deviation is below the response threshold.

When a sensitive element of this type is embedded in injection mortar the increase in pressure during the early hydration reaction causes constriction of the hollow tube. For the mortar used a maximum reduction in the tube diameter of 6 nm was estimated. This does not influence the strain signal because the deviation in contraction is less than 10^{-11} of the tube length. From a simulation of this pressure (hydrostatic pressure), an axial displacement of the end faces of the order of the threshold value was found. It could not be categorically stated that these changes were induced by pressure; temperature influences were taken into consideration.

When strain waves pass through the test object the sensor can also measure the dynamic wave field in terms of a strain field which modulates the cavity length. This causes an intensity modulation at the output of the sensor. By using this surface-mounted or embedded gage,

interference-free oscillations (including Fourier spectra) and acoustic signals can be recorded up to a range of 100 kHz.

Owing to the high resolution of changes in tube length, temperature changes produce a deformation as well as an output signal. It should be noted that the sensor measures the effective deformation under load induced by thermal expansion as well as by constraint. In order to assess the portion of the thermally induced strain, especially for measurements under constraint, the temperature has to be recorded separately and compensated by calculation.

SURFACE-MOUNTED SENSORS FOR MEASUREMENTS ON/IN LARGE CONCRETE STRUCTURES

In reinforced or prestressed concrete structures strain sensors are usually attached to the surface of elements or components of the structures

by bonding on the concrete surface, or
by bonding on embedded steel components (rebars, prestressing elements, tubes).

Sensor applications on the steel components of structures are discussed below.

Considerations with respect to the method of application

For applications involving fiber-optic microstrain sensors a number of issues with respect to the attachment of the hollow glass tube or sensing fiber portion to the surface of the component need to be considered:

handling of the sensor and preparation for its intended application;
choice of bonding agent and test of the bonding process;
preparation of the surface of the test object; and
design of the sensor to handle the expected loading range, temperature influences, alternating stress, etc.

The sensitive element is normally attached by means of an adhesive. This material has an indefinite thickness and an elastic modulus which differs from those of the sensor and the test object. When the test object becomes deformed, a strain/stress transfer occurs from the structural component to the adhesive layer as well as from the adhesive layer to the sensor.

This transfer is significantly affected by the thickness and the elastic modulus of the adhesive, and causes a shear stress in the adhesive layer. The adhesive, which does not follow Hooke's law, produces an unknown state of deformation. The engineer is confronted with the problem of interpreting the influence of the adhesive. The actual state of stress influences the accuracy of measurement. On the other hand, an appropriate dimensioning of the adhesive layer could enable the resolution and measuring range of the sensor to be controlled (cf. next section).

From a qualitative standpoint it follows that the thickness of the adhesive layer should be as thin as possible. From a calculation based on the solution of an elastomechanical boundary value case[2] with some approximations, it was be found that the shear stresses existing along the whole length of the applied sensor are concentrated at its ends. Therefore an almost complete strain transfer from test object to sensor can be expected. These problems are very similar to those experienced in the application of resistive strain gages (DMS). But the geometric dimensions and the mechanism of load transfer to the sensing area of the sensor are very different. The described fiber-optic microstrain sensors can be attached in two ways: either by complete attachment of the sensor tube or by attachment of both ends of the tube. The hollow tube has no coating.

Assuming that:
the bonding between glass tube and steel surface is chemically inert (no slippage and no gap) and
the strain field in the tube and in the test object is continuous, the sensor can be expected to detect uniaxial stresses only as a function of sensor length.[3] For our present investigations, transverse effects need not be taken into account; the sensor is only used in its sensitive (axial) direction (see above).

Laboratory tests

In experimental investigations at the IEMB the sensors were applied on different test samples (reinforcing steel, flat steel, square-sectioned rod of aluminium) in the tensile direction; dif-

ferent strain-transfer behavior was observed for different adhesives.

After carrying out a number of tests, and by using resistive strain gages for comparison, it was found that the completely attached fiber-optic sensor is best able to transfer load changes if the adhesive layer is thin. But the results obtained by the fiber-optic sensor and resistive strain gage showed a difference in terms of strain. Above a specific strain value — for this equipment above 16 $\mu\varepsilon$ — we observed a weaker increase in strain for the DMS. The percentage deviation measured was 13.8% for strain values above 35 $\mu\varepsilon$. This behavior was observed in all of our tests in the laboratory and on site. An example of a comparative test measurement is shown in Fig. 2. This remarkable effect can not be fully explained as yet. It should be regarded as an indication of the fact that fiber-optic strain gages have to be investigated further before they can become an established method like resistive strain gages.

Figure 2 illustrates the weak resolution of the resistive strain gage used for strain measurements; an uncertainty of measurement of 2.1 $\mu\varepsilon$ was obtained. By using an EFPI sensor the uncertainty of measurement was 0.52 $\mu\varepsilon$.

The use of a modified, stress-free fiber-optic microstrain sensor showed unexpected behavior compared with the stiffer sensors, even when materials with a relatively high elastic modulus were used. Figure 3 illustrates this behavior for flat steel equipped with several stiff and stress-free fiber-optic sensors. Transverse effects on strain were below the threshold of response (<0.08 $\mu\varepsilon$) and could not be detected. Comparable behavior for strain measurements was also found by Sirkis and Haslach[4] in experimental investigations.

In order to minimize the hysteresis an attachment over the full length of the sensor should be adopted as the preferred method. Measured values of hysteresis for an adhesive layer thickness of ≤ 8 μm are about 10 nm (absolute value related to the measuring basis of 10 mm). The hysteresis behavior of sensors attached at their ends does not seem to be as good. A systematic investigation needs to be carried out for this new technique.

Examples

An important step towards the ultimate success of fiber optics in civil engineering is their advantageous use on structures which have to be inspected urgently or — in addition to conventional methods — which have to be assessed with complete certainty.

The following examples, showing the advantages of fiber-optic microstrain gages when used for evaluating the static and dynamic behavior of structures, are indicative of the progress made in the development of adequate microstrain gages.

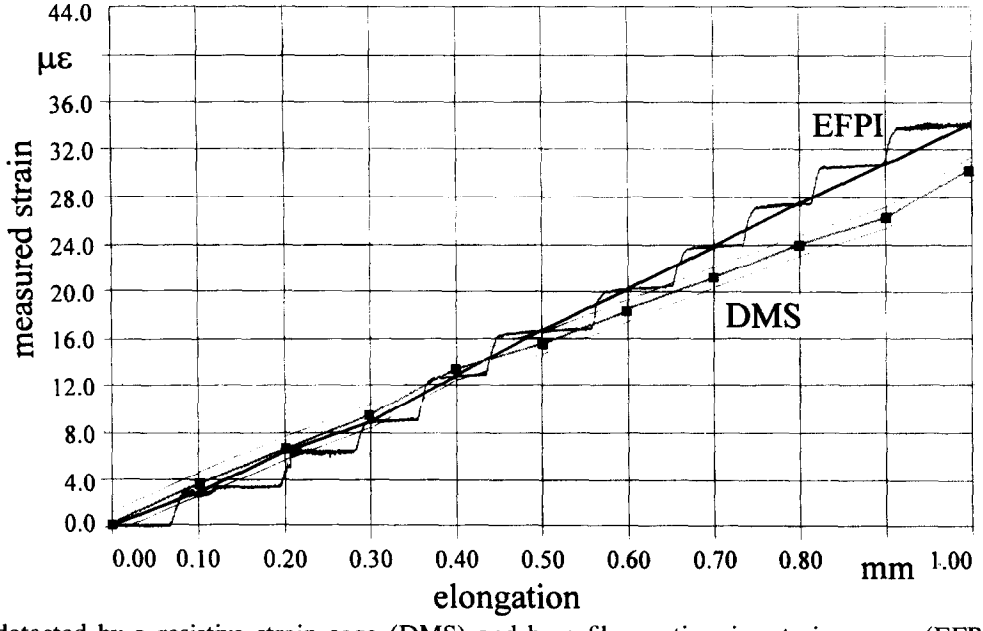

Fig. 2. Strain detected by a resistive strain gage (DMS) and by a fiber-optic microstrain sensor (EFPI) during elastic deflection of a reinforcing rod. Cantilever beam length: 350 mm; position of the sensors: at mid-span.

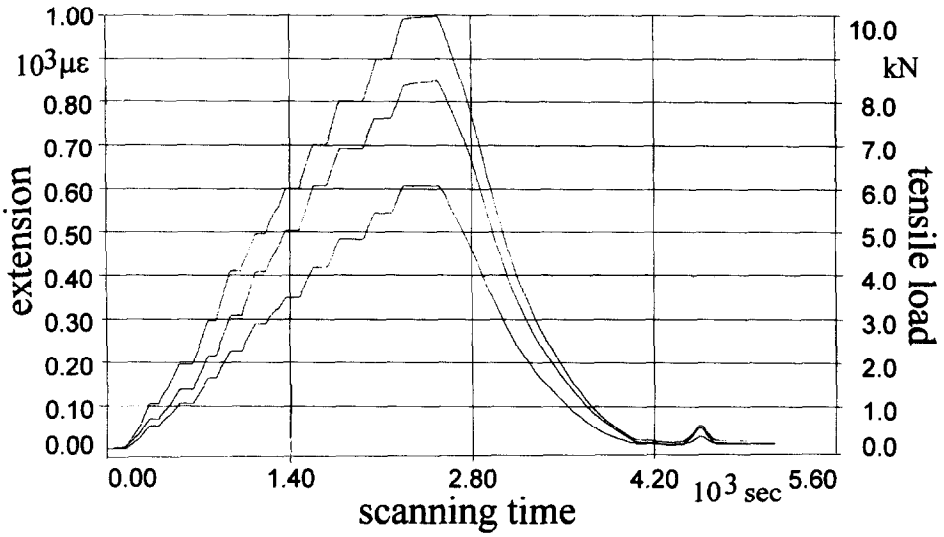

Fig. 3. Comparison of strain measured in a tensile test specimen by means of a dial micrometer (top curve), a stress-free fiber-optic sensor (center curve) and a stiff hollow-tube sensor (bottom curve, cf. Fig. 1). Sample: flat steel St 38, 20 mm × 4 mm; span: 480 mm.

Application in a box girder of a prestressed highway bridge in Berlin

A routine check of a motorway bridge in Berlin revealed a vertical crack at the outside of the bridge's box girder as well as several smaller cracks near the main crack. To assess the functional efficiency of the tendons, measurements concerning the vibration behavior, the deformation and the behavior in the cracked region had to be carried out. Several electrical sensors and fiber-optical sensors were used.

On both sides of the crack region one of the tendons was opened and a fiber-optical microstrain sensor as well as a resistive strain gage were applied to an exposed steel wire of the tendon (Fig. 4). For this first installation of a fiber-optic microstrain sensor on a prestressed concrete bridge in Germany (1993),[5] ferometer sensors (EFPI; manufactured by Fiber and Sensor Technologies, Blacksburg, Virginia, USA) were used.

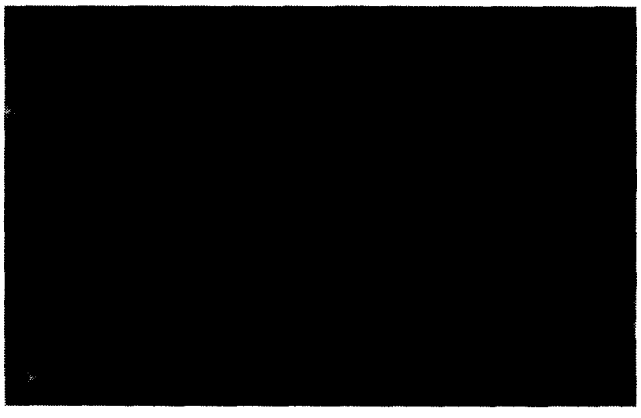

Fig. 4. Fiber-optic sensor attached to the exposed steel wire of a tendon.

Instrumentation and data acquisition

Strains from the resistive strain gauge and the EFPI were acquired by receiving devices. For the micro sensors a special bias and receiving device (manufactured by Fiber and Sensor Technologies, Blacksburg, Virginia, USA) was used. The electronic signal was digitized (A/D transducer width: 12 bit) following conversation and amplification. A commonly available data processing program was used to record and evaluate the strain signals.

An uninterrupted power supply (UPS) was connected to the supply circuit of the data-recording equipment as a safeguard against power failure (max. 3 h) and voltage peaks. Filtering of data and preliminary data editing were not intended, i.e. raw data were stored on the hard disk of the PC (486 MHz, hard disk: 240 MB) as original signals.

The interferometric sensors were sampled at 100 Hz for the test loads and at 200 Hz for the traffic loads.

Proof testing. A DEMAG AC type 435 motor crane (5 axles, uniform axle spacing of 1.5 m) with a total weight of 66 ton was used for loading. The motor crane drove at different speeds (idle speed, 30 km/h, 60 km/h) on different lanes of the bridge. In addition, responses from

typical traffic loads, including a large number of trucks, were recorded.

Results. Resolution of nearly 0.05 $\mu\varepsilon$ (on site only valid for short-time measurements) made it possible to record both the static and dynamic response of the bridge (by recording the strain in tendons under proof loading and traffic loading) by a single EFPI sensor. Figures 5 and 6 depict the high performance of the EFPI sensors. It should be noted that the existing electromagnetic interference did not influence the measured values. The natural frequency of the bridge, $f_r = 2.10$ Hz, and the damping ratio of $\beta = 1\%$ can be easily derived from Fig. 6 by looking at the final oscillation curve of the bridge at the instant of vehicle exit from the bridge.

The fundamental oscillations of the bridge during traffic hours (Fig. 7) was $f_t = 2.06$ Hz, which is in good agreement with the natural frequency measured in the absence of traffic. An additional finite-element simulation of the static and dynamic behavior of the prestressed concrete bridge showed a very good correspondence between static (strain) and dynamic (natural frequency) responses.

Following the proof tests, the exposed sections of the prestressing tendons were repaired, and the sensors were kept in place for future monitoring activities.

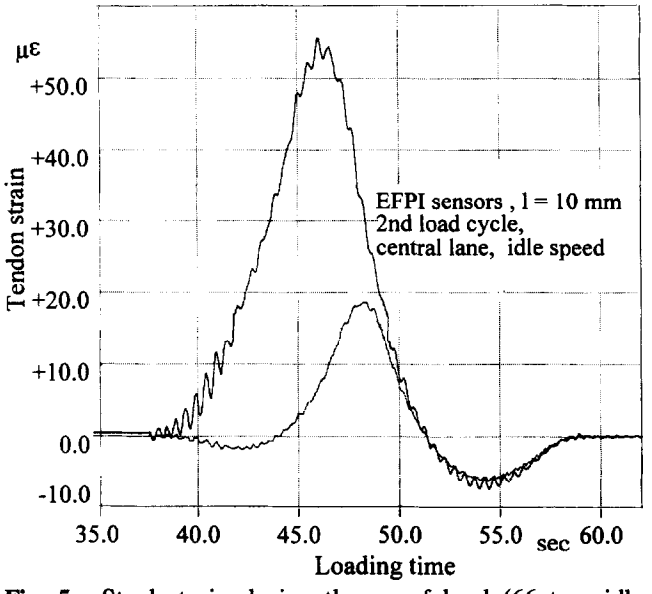

Fig. 5. Steel strain during the proof load (66 ton, idle speed). Smaller deflections: sensors placed at the calculated zero-moment point of the bridge.

Application of fiber-optic microstrain gages inside a concrete pile

The deformation behavior of concrete piles is normally determined by resistive strain gages applied on the concrete surface or on the rebars inside the pile. Manually operated sliding micrometers are used to assess the deformations in sections along the pile.

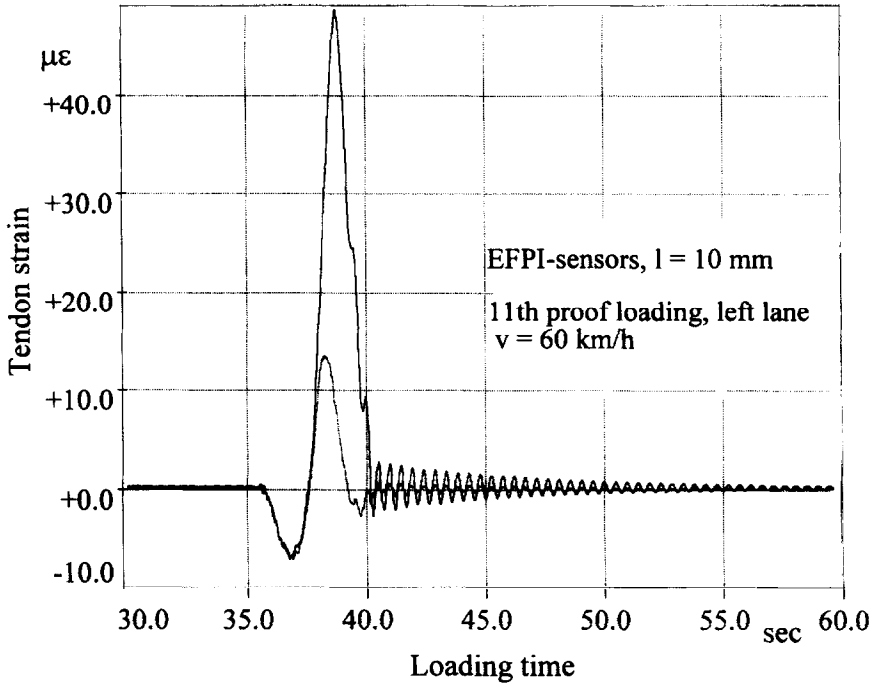

Fig. 6. Steel strain during the proof load (66 ton, 60 km/h).

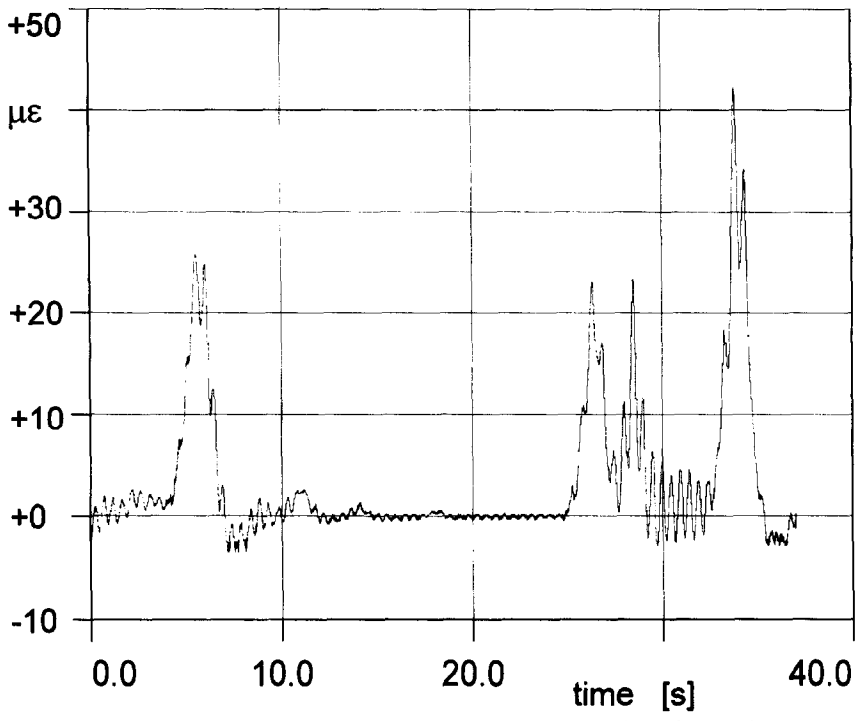

Fig. 7. Typical traffic load, including a large number of trucks (peaks allow identification).

Instrumentation. To simplify the manual measuring operation using sliding micrometers one should take the opportunity to use sensor fibers spanned inside the pile for on-line data scanning. These sensors can be installed in the reinforcing cage and can be attached at fixed intervals. Furthermore, one should apply highly resolvable EFPI sensors in addition to, or instead of, resistive strain gages for recording static and dynamic events.

Pile tests were carried out at IEMB in cooperation with the Foundation Engineering Department of the Technical University of Braunschweig. A reinforced concrete pile of length 2 m was equipped with different sensors.[6] A series of axial compressive loading and of dynamic measurements was conducted (Fig. 8).

In addition to the conventional sensors, the following fiber sensors were applied:

an EFPI sensor, adhered to a circular rod (hooped reinforcement) for assessment of the lateral strain during compression of the pile (recording of the tangential component of deformation); and

a sensor fiber (prestressed stranded-fiber sensor of SICOM-type), length = 2 m, parallel to a sliding micrometer tube, i.e. very close to the pile axis.

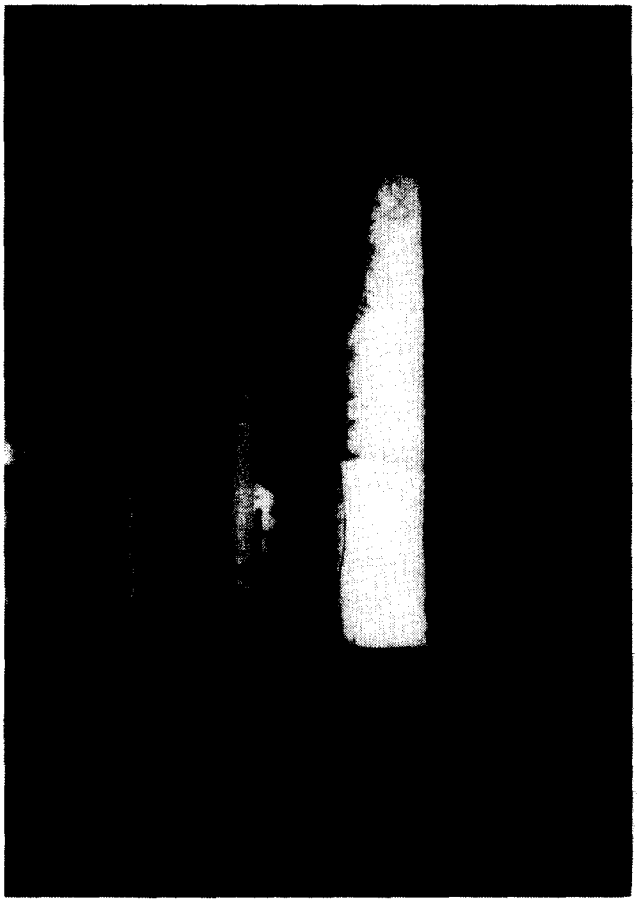

Fig. 8. Pile placed in the compressing frame of the IEMB.

The operational principles pertaining to the above-mentioned sensors are given in elsewhere.[7] The stranded-fiber sensor works on the microbending principle. In addition to the computer-linked sensors a dial micrometer and inductive displacement meters were installed outside the pile (Fig. 9).

Figure 10 shows results from vertical compressive loading of the pile. Load levels were at 100, 400, 800 and 1200 kN. Results from the four EFPI sensors (resolution 0.1 μm/m) indicated that the pile had developed lateral buckling during loading. Results are in good agreement with those obtained by the conventional methods. They demonstrate that computer-aided scanning of pile deformations by means of fiber-optic sensors can be achieved without difficulty and with high accuracy. The additional possibility of using a sliding micrometer could enable a periodic check of stranded-fiber sensors as part of a long-term monitoring process.

Fig. 9. Instrumentation of the reinforcing cage of the concrete pile.

SENSOR INSTALLATION INSIDE A LARGE CONCRETE WALL

In large concrete structures newly poured sections need to be built up successively upon already hydrated concrete sections. In such cases, physical constraint in the fresh concrete during curing, caused by differential temperature variations in both concrete sections, can lead to cracks. These cracks, e.g. in the construction of sedimentation basins, cause leaks. Therefore reinforcement is provided for the purpose of crack control of restrained concrete components (according to the German and European standards, DIN 1045 and EC 2, respectively).

In order to assess the effectiveness of a combined heating and cooling process in the construction of settling tanks, with the aim of reducing cracks, the thermally induced deformation of a reinforced concrete wall was monitored during hardening of the concrete. For this purpose a number of strain sensors were mounted in the reinforcing cage and placed in operation before casting the concrete sections.[8] Sensors had to resolve the measured data to less than 1 $\mu\varepsilon$ and to record it for several weeks. The basic sensing element is shown in Fig. 1.

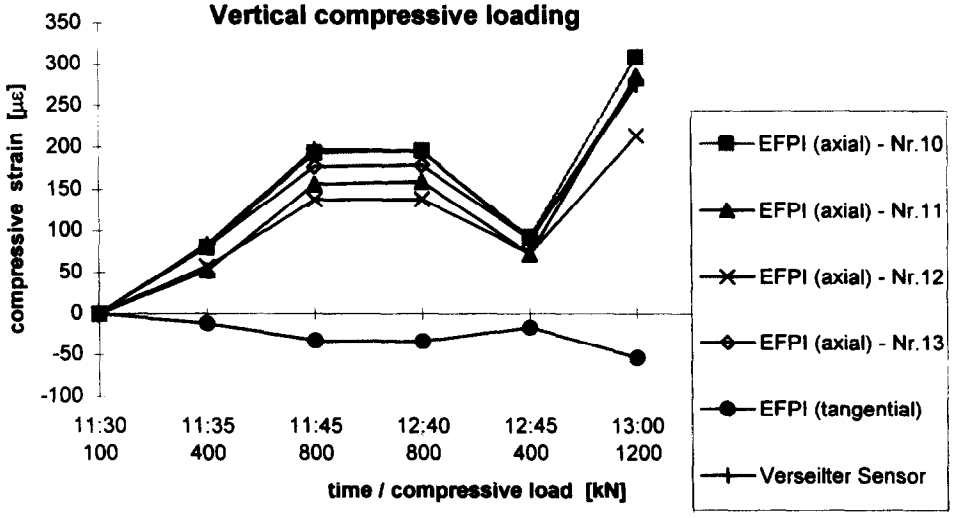

Fig. 10. Deformation of the pile as a result of vertical compressive load, measured by fiber-optic sensors.

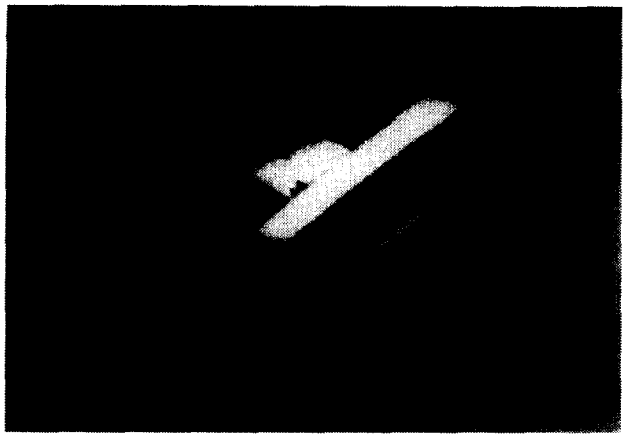

Fig. 11. Sensor head with 'ears' embedded in a silicon rubber material.

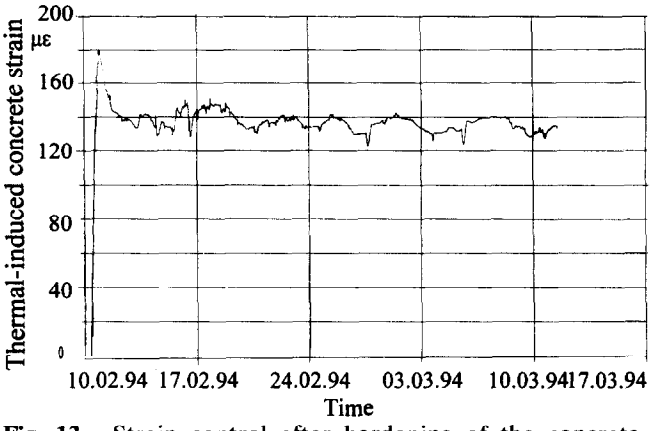

Fig. 13. Strain control after hardening of the concrete wall.

Two kinds of strain probe were used: a sensor tube with 'ears' coated with a thick layer of silicon rubber (type a), and a fiber-optic microstrain gage (type b).

Type a: sensor tube with 'ears'

Sensors were embedded in a protective material (silicon rubber). Two thin metal strips ('ears') were attached to the sensor head body so that the ears protruded from the silicon rubber (Fig. 11). This protected sensor was embedded in prism of a cement mortar (4 cm × 4 cm × 16 cm) to which its ears clinged. The connected cable was protected in the mortar body by a flexible armour tube of steel to prevent damage during pouring of the concrete.

Load transmission from the mortar to the sensitive element showed a satisfactory linearity. Figure 12 illustrates a calibration curve for one of the sensor probes used. However, this kind of sensor head showed weak sensitivity. Since the loss of these sensors was still acceptable, and with a view to the calibration curve in the expected measuring range, it was possible to use this design for the measurements.

Figure 13 shows the thermally induced deformation measured in the concrete wall of the settling tank.

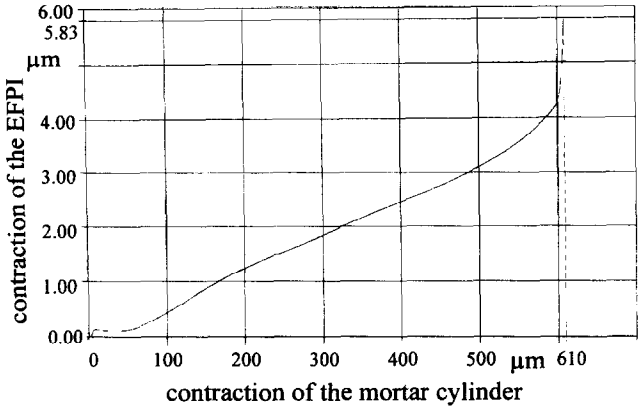

Fig. 12. Calibration curve for the sensor shown in Fig. 11. (The linear transmission range of the sensing arrangement, correponding to a mortar contraction from about 50 μm to 570 μm, is limited by the mechanical transmission system chosen for this task.)

Type b: fiber-optic DMS

To improve the load transmission for a further measurement on the building site, the fiber-optic sensor was attached to a steel bar of quadratic cross-section with anchor plates on both its ends. This was done in accordance with a method commonly used to measure concrete deformation by means of resistive strain gages (Fig. 14). In order to rule out inaccurate measurements due to deflection of the steel bar during deformation of the concrete, the strain gages were applied on opposite faces.

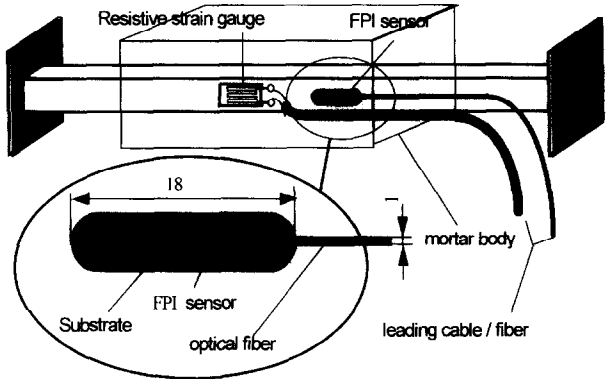

Fig. 14. Fixing of the resistive and the fiber-optic strain gages on the steel bar.

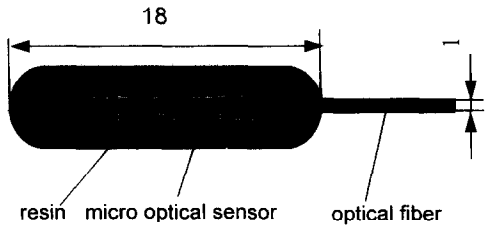

Fig. 15. Detail of Fig. 14: fiber-optic microstrain gage comparable to a resistive strain gage (thickness of the gage: 0.8 mm).

For this application on a steel bar the fiber-optic sensor was prefabricated by embedding it in a specially modified methyl methacrylate resin (Fig. 15) in order to ensure appropriate compatibility with the adhesive material used. Next, this sensor tip was attached along its full length, by analogy to resistive strain gages.[9]

Figure 16 shows the calibration curve of one such fiber-optic strain gage. This type of application leads to a strong improvement of the load transfer compared with the microstrain sensor embedded in silicon rubber. In this case the medium between the steel and sensor tip is merely an adhesive varnish layer of a few μm thickness. This is very important because a thicker resin layer can influence the load transfer between the test object and sensor indefinitely.

The fiber-optic strain gage was protected only by a thin layer of a special alkali-resistant adhesive varnish. This application has the advantage that electric contacts inside the mortar body are avoided. While the durable protection of resistive strain gages consists of a multi-layer protection against diffusing moisture, which itself influences the measuring results, this precaution was not necessary for optical sensors.

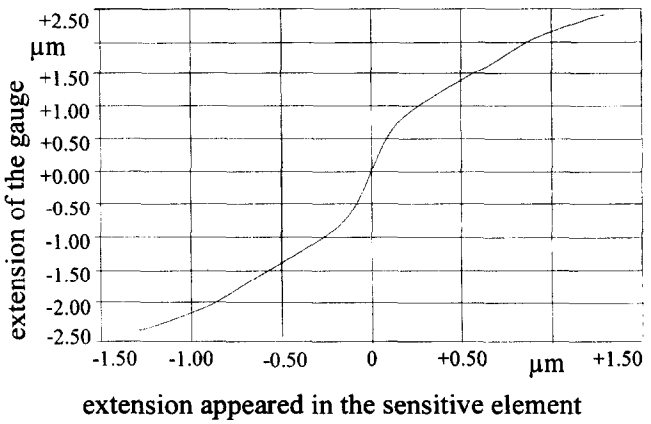

Fig. 16. Calibration curve of a fiber-optic strain gage shown in Fig. 15.

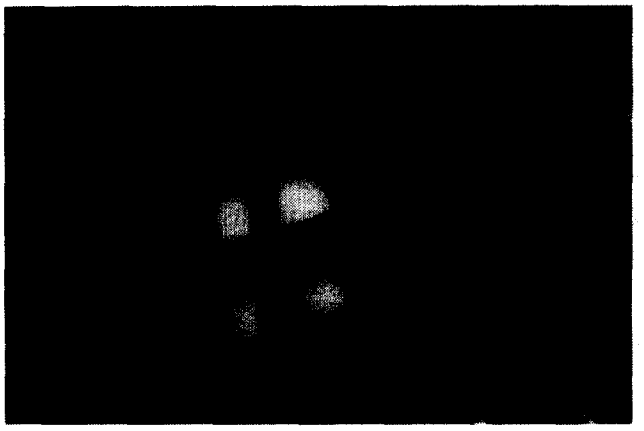

Fig. 17. Installation of sensor bodies in reinforcing cage of the wall.

Figure 17 shows the position of two of the measuring rods mounted in the reinforcing cage of an activated sludge basin wall.

The major advantage of the described fiber-optic sensors was the fact that they were able to measure the thermally induced concrete deformations with a very high resolution. But the method used has two drawbacks, as follows.

At the current stage of development, the reproducibility of the substrate material in which the sensing element is embedded is not yet satisfactory. Each sensor gage has to be calibrated in the laboratory, and thermal influences as well as stresses, especially in the substrate material, cannot be avoided.

The measuring arrangement described above causes load concentrations at the mortar prism generally used, as a consequence of shrinkage of the surrounding concrete. This is a serious problem. A correct and reliable measurement of very small concrete deformations, in order to reveal cracking at an early age of the concrete, is not possible.

For this reason, it is necessary to find a stress-free sensing arrangement, to design a strain probe (similar to a pencil) and to find a way of embedding such sensors directly, without any heavy and disturbing covering, during the casting operation. As an alternative, sensor heads with very small dimensions (probe volume <1 cm^3) should be used. In this way deformations could even be recorded in the viscoelastic phase of the mortar/concrete, as well as later on, without impairing the behavior of the test object. Consequently, one has to avoid making the test object stiffer than it would be without the sensor.

The following section contains a discussion on problems relating to the embedment of fiber-optic microstrain sensors and presents preliminary data showing the material behavior at the early ages and later on, under different influences, obtained by means of unprotected sensors embedded directly in the mortar, without disturbing the measuring environment.

EMBEDDED SENSORS FOR MEASUREMENT OF MORTAR AND CONCRETE DEFORMATIONS

Highly-resolvable sensors will become very important instruments for assessing the hardening behavior of mortars and concretes. Such sensors are needed in the process of condition monitoring of buildings, as well as for scientific investigations of different mortar compositions.

The use of ordinary sensors to measure deformation behavior of mortar or concrete is very difficult or virtually impossible. An embedded sensor disturbs the behavior of the test object. This is problematical when deformations of extremely low strength mortar or concrete are to be measured. All existing sensors alter the stiffness of the material compared with plain mortar. This gives incorrect results.

The fiber-optic micro sensors tested and further developed in the fiber-optic laboratory of the IEMB, especially the new non-reactive microstrain sensors, are designed to enable non-destructive measuring of the mechanical properties of young concrete and of other building materials, i.e.:

measurements of deformation of hardening concretes in different mixtures;

measurement of reactions under the influence of heat and moisture, as well as under sulphate-induced expansion; and

measurement of load-induced and creep deformations on structural components.

Compatibility of sensor in the host material: durability of the sensor

Prior to embeddment of the relatively vulnerable microstrain sensors in cementitious materials, a number of different issues relating to the sensor design have to be addressed:

how to design the sensitive elements in order to obtain reliable bonding to the matrix and

how to ensure stable operation in the long term.

Very practical questions have to be answered as well:

how to protect these sensors against damage resulting from contact with aggregates and

how to prevent damage to the sensor resulting from the high alkalinity of the mortar/concrete.

First, it is obvious that the glass tube of the sensing element and the leading fiber have to be protected against mechanical and harsh chemical influences by means of an appropriate coating material. To assess the behavior of optical fibers directly embedded in cementitious mortars and concretes, both conventional as well as customized fiber coatings were tested.

Six differently coated optical fibers (see Table 1) were immersed over different periods of time in alkaline solutions:

aqueous, saturated concrete extract, pH = 11;

Table 1. Specification of fibers used

Designation	*Glass type and dimensions* (d_i/d_o *in* μm)	*Coating*	
		Thickness (μm)	*Material (construction)*
0-1*	G, 50/125	62.5	Acrylate system (colour-coated)
0-2*	G, 50/125	32.5/30·0	Acrylate system (inside: soft/outside: hard)
0-3	S, 9/125	62.5	Acrylate system
0-4	G, 50/125	7.5	Polyimide
0-5*	S, 50/125	14.8	Polyimide (colour-pigmented)
0-6*	G, 200/220	11.5	UV-hardened HPCS (fluorine polymer)

*These types were embedded in concrete.

Fig. 18. Test arrangements: top, conditioning of fiber samples in aeqeous alkaline solutions; bottom, mortar bodies for investigation of embedded fiber samples.

saturated $Ca(OH)_2$ solution, pH = 12.4;
soda lye, 3%, pH = 14; and
potash lye, 3%, pH = 14.

After 1 day, 7 days, 21 days and 5 months (separate vessels, Fig. 18) the samples were visually assessed and studied by means of scanning electron microscopy (SEM) with regard to attack by hydroxyl ions and several cations. Four types were embedded in cement mortar bodies (right parallelepiped specimens, 160 mm × 40 mm × 40 mm, Portland cement PZ 35 F) and moderately tamped. After 28 days they were analysed by SEM and by micro sectioning.

The aggregate grain size and mix proportions by weight of constituents were varied as follows (c: cement, a: aggregate, w: water):

First test series—aggregates: sand ≤ 1 mm with 15% crushed stones 1–4 mm; c:a:w = 1:3:0.46

Second test series—aggregates: sand ≤ 1 mm; c:a:w = 1:2:0.63.

Compaction was carried out manually (first test series) and dynamically with 30 Hz for about 2 min (second test series). Compaction was terminated as soon as air bubbles no longer appeared on the mortar surface. The mortar was not poured too carefully in order to roughly simulate the conditions on site. The fibers protruded at the end faces of the bodies; these were stored for 28 days. Exposure of the fibers was achieved by means of a PVC shim which ended about 3 mm above the fiber line (Fig. 18). After pulling out the shims the bodies were carefully split into two; the fibers could be analysed very well. Damage resulting form the procedure of uncovering the fibers was ruled out by means of comparative assessments of a large number of samples.

Fig. 19. Polyimide-coated fiber (type 0-4) conditioned in sodium lye (3%, pH = 14) for 7 days.

All inspections were made at room temperature. Figure 18 shows the test arrangements. In general, the chosen polymeric coatings are considered to be resistant to alkaline solutions. We realized that all investigated coatings more or less changed their properties when conditioned in alkaline solutions or embedded in cementitious mortar.

Polyimide coatings

When conditioned in NaOH, polyimide coatings exhibited changed behavior even after 24 h. Figure 19 (type 0–4) shows a softened coating after 7 days which results in crinkling and peeling of parts of the coating. The same coating type (fiber type 0–5) embedded in a mortar body with a w/c value of 0.46 and investigated after 28 days shows a similar behavior. Figure 20 shows crinkles resembling expansion bellows, as can also be observed in alkaline solutions. Cement paste has become deposited between the crinkles of the coating.

From a micro section of the embedded fibers we obtained a more detailed view of the coating. There are small bubble-like zones distributed on the whole coating surface. These zones were formed in the boundary region to

Fig. 20. Polyimide-coated fiber (type 0-5) in cement mortar (28 days; w/c ratio: 0.46).

the mortar; they did not reach through to the glass fiber. The micro section also showed a crack through the coating, probably caused by some kind of swelling of the fairly hard coating during the hydration reaction. In general, we found a good stability of polyimide-coated fibers embedded in cementitious mortar materials compared with other coating materials.

Fluorine-containing thermoplastic coatings

Thermoplastics containing fluorine are supposed to be permanently resistant to alkali. We observed no influence of any kind owing to alkaline attack for 21 days. But after conditioning in saturated concrete washout solution for 5 months, the same samples no longer showed a smooth surface. We also found this on fibers embedded in cement mortar. We found concentric deformations which could not be detected in the case of unloaded fibers. The micro sections showed clear swelling-like changes and deformation (Fig. 21) compared with fibers that were not exposed to mortar (e.g. embedded in epoxy resin). The UV-cured fluoropolymer coatings were obviously swollen as a consequence of the alkaline environment. An estimation of changes in the hardness of coating type 0-6 is not possible, although some difficulties in making the micro sections pointed to softening of the coating.

Acrylate coatings

Acrylate-coated fiber surfaces conditioned in $Ca(OH)_2$ developed matt patches ('emery paper effect') after 21 days. The same effect could also be observed on fibers conditioned in concrete washout solution. We observed a good bond between the coatings and the matrix. However, investigations of these fibers by SEM revealed several cracks with a width from 870 nm to 2 μm along the unprotected fibers (Fig. 22). Beside the cracks we found strips resembling cracks, obviously caused by strain deformations in the coating when it was uncovered. All samples showed these 'strips'; on some samples we found only local 'swollen' regions with crack-like strain deformation zones (furrows). It is not possible to determine whether these surface flaws are related to damage of the coating during the embeddment process.

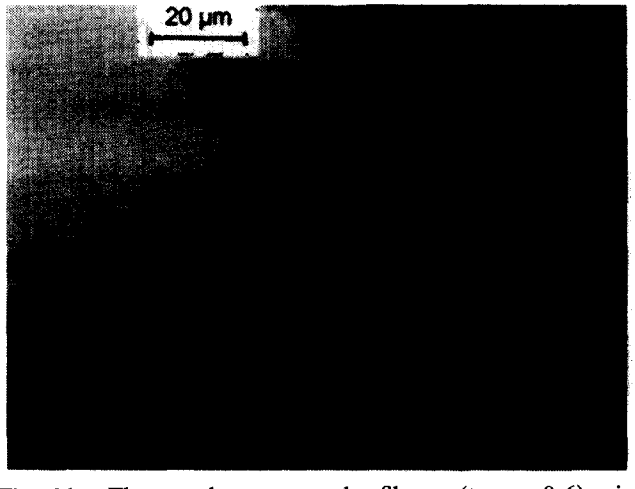

Fig. 21. Fluoropolymer-coated fiber (type 0-6) in cement mortar (15 days; w/c ratio: 0.63).

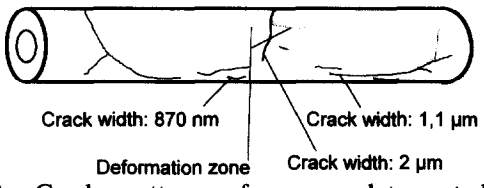

Fig. 22. Crack pattern of an acrylate-coated fiber embedded in cement mortar (28 days; w/c ratio: 0.63).

A more detailed description of our investigation and findings is published elsewhere.[10] Learning from these investigations, we manufactured sensors with specially chosen coatings for embedment in different mortars. A selection of results is presented below.

Consideration of the influence of the coating in the sensor/matrix boundary region: load transfer

The following considerations assume a homogeneous coating layer for a better estimation of its influence. This is not really valid when the coating is treated for a good bonding behavior.

The strain and stress transfer behavior can be adjusted by means of the coating layer. The design of the coating (thickness, elastic modulus) allows strain and stress concentrations to be shifted to the sensor/coating or coating/matrix boundary. The measuring task has two objectives:

measurement of deformation/stress in a very soft environment (i.e. in the plastic phase of a young mortar); and

measurement of deformation/stress in a matrix with increased modulus of elasticity (i.e. in matured, hardened mortar or concrete).

It is obvious that case 1 is more difficult to measure because the deforming plastic mortar cannot work against the restoring force of the stiff sensor. The force transfer from mortar to sensor is effected by the coating. The differences between the strain of the matrix and that of the coating lead to shear stress in the matrix (an adequate force transfer resulting from good bonding between coating and matrix is assumed). Mathews and Sirkis[11] have calculated that a ratio $E_M/E_C > 10$ leads to significant stress in the matrix, which influences the measuring result.

In order to obtain a good strain transfer from the matrix via the coating to the sensor, the influence of the coating elasticity (including strain losses) must be estimated. At the same time, stress and strain concentrations at the coating boundaries of the sensor and matrix must be known. The following estimations have been made within the context of investigations by Mathews and Sirkis[11] and Pak[12] for embedment of fiber sensors in composites.

Case 1

A coated sensor embedded in fresh mortar has a higher elastic modulus G_C (where C stands for 'coating material') than the mortar (cement paste). For this case $G_C > G_M$ (where M stands for 'matrix material') and strain concentration is produced at the coating/sensor boundary, and one can assume a weak stress reaction to the viscoelastic matrix material. For a better strain transfer the coating material should not be too thin. It follows from a simplified shear stress analysis applied to the coating boundaries[13] that maximum shear transfer is reached when the shear modulus of the coating G_C is the geometric mean of the shear moduli for G_S (where S stands for 'sensor material'; here, glass) and the matrix G_M (true for all coating thicknesses):

$$G_C = \overline{G_M G_S} \tag{3}$$

A good choice for the coating would be a time-dependent increase for G_C because the value G_M of fresh mortar is a function of time, $G_M = f(t)$:

$$G_C(t) = \overline{G_M(t) \cdot G_S} \tag{4}$$

However, the best way to measure the volume changes of a very soft mortar matrix is by use of a sensor with an extremely low stiffness.

Case 2

Stress concentrations in hardened matrix material are not problematic for a stiff sensor (shown in Fig. 1). A shear modulus ratio of $G_M/G_C \cong 1.7–3.2$ can be assumed for sensors with polymer coatings embedded in matured mortar. The maximum stress shifts from the coating/sensor boundary to the coating/matrix boundary. (A softer coating acts as a cavity inside the mortar.) The best strain transfer can be achieved with a very thin coating.

Bonding behavior: slippage/load transfer

Good bonding is not only important in load-bearing composites ('strengthening effect') but also for reliable load transfer in embedded sensing fibers.

The bonding behavior is mainly influenced by the type of coating material chosen, which determines the microhardness of the interfacial zone around the sensor. One coating type can lead to an increase of the hardness of the interfacial zone, another one keeps this region soft. From earlier investigations carried out in the 1980s[13] we know that a coating made from carbon with poly(vinyl acetate) should ensure a good bond to a cement paste matrix. A very interesting method to get good bonding behavior is the choice of an epoxy resin (including an appropriate hardener) which causes some interactions with the pour solution of cement paste, resulting in a dense (hard) interfacial region. Conversely, a soft coating is not appropriate for getting adequate load transfer.

Experimental results

We embedded microstrain sensors coated with different polymeric materials and with a very thin carbon layer (< 1 μm) in different types of mortar. For a preliminary assessment of the coatings which are to be chosen for embedment, we used the method of micro sectioning of embedded sensors. Figures 23 and 24 show a selection of our present results.

The cross-section of the described Fabry–Pérot-type fiber sensor (Fig. 1) can be easily recognized. The bond between the inorganic coating (carbon layer) and the cement mortar matrix makes a satisfactory impression (Fig. 23).

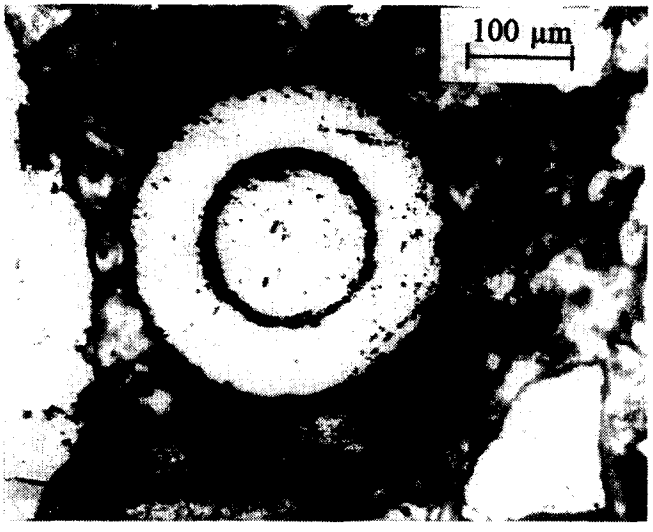

Fig. 23. Micro section of a carbon-coated microsensor embedded in cement mortar (grain sizes: 0–4 mm; curing period: 8 months).

This is also reflected in relatively good measuring results (cf. Fig. 29).

An interpretation of the micro sections of polymer-coated sensors is more complex. Depending on the material chosen we found a different appearance of the interfacial region. Figure 24 shows a sensor coated with a specially adapted poly(methyl methacrylate) material. Because of the irregularity of the surface, it showed good gripping behavior to the mortar (cf. curve of polymer 2 in Fig. 29). However, in this embedment case we observed a strikingly large number of additional pores in the interfacial zone around the fiber. This is obviously caused by an interaction between the laitance and the polymeric material in a very early phase

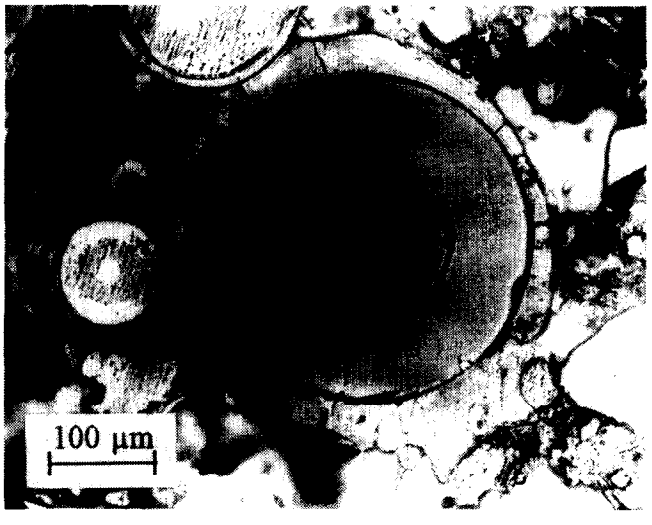

Fig. 24. Micro section of a polymer-coated microsensor embedded in cement mortar (grain sizes: 0–4 mm; curing period: 8 months).

of the hydration reaction (we also found these additional pores in micro sections of some other specimens with polymeric materials, but not in each case). The cracks in the coating layer could be caused by stress during the shrinkage process of the hardened mortar. Until now, we could not find an adverse affect on the glass material.

The investigations are yet complete; other samples are currently being tested. However, it already seems that optical fibers embedded in mortar with aggregate grains of a size <1 mm in diameter will not be touched by these. In all our investigations we did not find any contact between coating and aggregates.

Macroscopic discussion of the influence of sensor design on strain transfer in mortar; sensor probe

Normally, the stress and strain distribution in concrete is very heterogeneous. This fact requires the use of the greatest possible sensor length for strain measurements. As an orientation, Rohrbach[14] recommends keeping to a ratio of

$$V = \frac{l_m}{d_m} \geq 10 \tag{5}$$

where l_m is the measuring basis of the sensor and d_m the medium diameter of the largest aggregate grain size. For $V \geq 10$ the maximum variation of the measured strain from the average is less than 5%. With regard to the sensors used, which have a typical measuring range of 10 mm, satisfactory results for mortar with a grain size from 0 mm to 1 mm can be expected.

Furthermore, the importance of the ratio of sensor length L to its diameter d_S (coefficient of finesse) should be stressed. According to Ref. 14, a homogeneous and elastic behavior of the hardened mortar, consisting of aggregates ≤ 1 mm in diameter, will be assumed for further estimation. This assumption is not valid in the strict sense because mortar shows heterogeneous behavior like concrete and because it strongly changes its elasticity at an early age, and also to a great extent during the process of maturing as well as under service load.

For a cylindrical sensor of length L and diameter $2r_S$, with an elastic modulus E_S and a Poisson's ratio μ_S embedded in a mortar prism

(E_M, μ_M, ideally infinite dimensions), a stress σ_S develops on the sensor surface, differing from the stress σ_M in the undisturbed mortar:

$$\sigma_S = \sigma_M(1+C_\sigma) \quad (6)$$

Because the sensor is a foreign body and hampers the strain, the mortar strain, ε_M, differs from that of the sensor, ε_S, as follows:

$$\varepsilon_S = \varepsilon_M(1+C_\varepsilon) \quad (7)$$

C_σ and C_ε are correction factors which characterize the difference in stress or strain for embedded sensors. In Fig. 25 the strain correction factor $(1+C_\varepsilon)$ is plotted as a function of E_S/E_M. From Fig. 25 we learn that, for an increasing ratio of L/r_S, no strong influence occurs when differences exist in the moduli of elasticity E_S (sensor) and E_M (mortar). Leaving apart the coating of the micro optic sensors (not really tolerable because of the coating elasticity E_C), a ratio $L/r_S \cong 50$ for the micro optic sensors (shown in Fig. 1) can be achieved. So a very weak influence of the elastic moduli E_S and E_M on the strain correction factor must be expected. It should be noted that the sensors are embedded directly in mortar, without any additional covering.

The favorable ratio $L/r_S \cong 50$ cannot be utilized when the fiber-optic sensing element is protected by a mortar body with approximate dimensions of about 20 mm long and 5 mm in diameter. For this arrangement we get a coefficient of finesse of $V \cong 4$. The influence of the difference in the elastic moduli on the strain correction factor $(1+C_\varepsilon)$ increases: stress is produced in the sensor/matrix boundary region. In this case, measuring rods with an artificially extended measuring basis should be manufactured; the resolution must not be reduced by this manipulation.

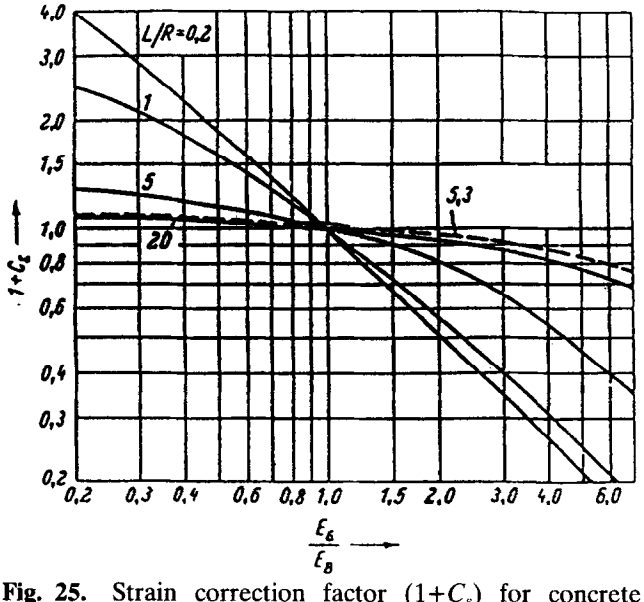

Fig. 25. Strain correction factor $(1+C_\varepsilon)$ for concrete sensors.[14]

Additional thermal stress due to different coefficients of expansion α_S (glass material of the sensor) and α_M (mortar matrix) is not considered here. However, for a correct analysis, especially for deformation measurements during the hydration reaction, this must not be neglected.

Conclusion from theoretical considerations: design rules?

It can be concluded that the measurement of deformations and stress variations (also residual stresses) in mortars and concretes in the phase of early hydration reaction and at an older age need to be accomplished by two sensors with differing dimensions. In practice, the engineer is confronted with limitations in the choice and design of appropriate coatings, but if fundamental knowledge about micromechanical interactions between sensor and matrix is available, design rules can be stated. In this way, incorrect measurements or variations in interpretations of the measured values will be prevented.

First experimental results in the measurement of micro deformations[15]

In accordance with the above considerations we used different sensor types for measurements of volume changes of young mortars and of matured mortars. Our experimental results confirmed the theoretical assumptions. The developed stress-free sensor type is able to measure mortar deformations in the elasto-plastic stage of the hydration reaction; it could not reliably measure strain/compression deformations in old mortar.

In order to record deformations in completely hydrated mortars caused by external mechanical loads, by temperature-induced volume changes or by moisture variations, the well-known type of stiff sensor coated with specially chosen materials was used.

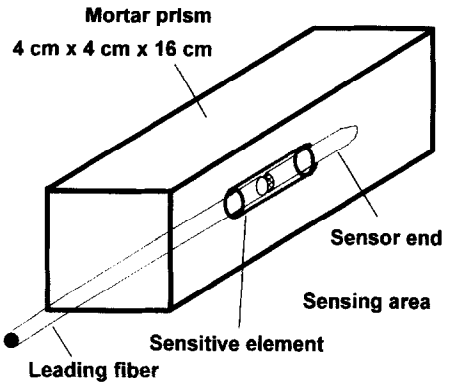

Fig. 26. Microstrain sensor embedded in a specimen (schematically).

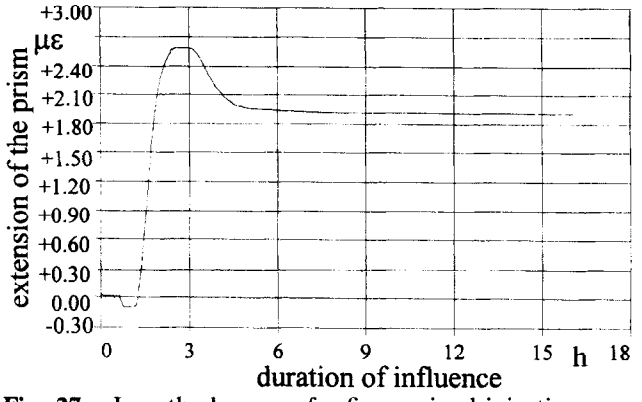

Fig. 27. Length changes of a fine-grained injection mortar (0 to 2 mm) during the hardening process (mixed according to the producer's instructions). Ductile density of the fresh mortar: 2.3 kg/l; room temperature: 26°C; sensor type: stress-free extrinsic fiber interferometer sensor (SF-EFPI).

The embedment of all types of microstrain sensors was carried out without any additional covering. The coatings were put on in our laboratory. On some samples the coating was treated with the aim of achieving a better bond. The very small fixing element used to hold the sensor inside the mortar did not influence the function of the sensor and was only used during the pouring procedure of the building material. Figure 26 schematically shows the position of the sensor in a specimen.

On-line measurement of length changes of mortar prisms at early ages

As an example of the high performance of embedded fiber-optic microstrain sensors, the results of measurements of the shrinkage and swelling behavior of an injection mortar within the first hours after casting will be presented. For this purpose we used stress-free arrangements of Fabry–Pérot fiber sensors developed by our group.

As test specimens we used standard prisms (4 cm × 4 cm × 16 cm). After casting the mortar into the standard mold it was covered with a steel plate. The steel plate was braced with the mold, and the web at the end face of the prism was movable. In this way, the increase in volume is forthcoming in longitudinal direction, i.e. mainly in the sensing direction of the tube. Figure 27 shows the contraction and expansion of the mortar within the first 16 h after casting. About 45 min after casting we could clearly observe a contraction of the mortar, and at 70 min after casting we recorded a considerable expansion. This swelling continued for about 60 min. Then followed a small shrinkage of about 0.7×10^{-3} $\mu\varepsilon$. After 6 h the sensor recorded no further deformations. The results had a resolution of 0.08 $\mu\varepsilon$.

Stiff sensors also embedded in the prism did not yield any reliable results in the plastic phase, as expected.

On-line measurements of load-induced length changes of matured mortars

On account of the requirement of $G_C < G_M$, the variety of possible designs for the coatings is quite large. Several coatings were investigated; some selected results are given below.

Figures 28(a) and (b) show the measured deformations of a 63 day old mortar prism and of a 46 h old prism under compressive load in a testing machine. The load levels were controlled by means of a dial micrometer; the compressive force was directly read on the machine.

A number of tests confirmed that the choice and the treatment of the different polymeric coatings (for bonding improvement) as well as the method of embedment are decisive for the effectiveness and the linearity of the strain transfer from test object to sensor. Figure 29 compares the strain vs compressive loads measured by several differently coated and treated microstrain sensors, embedded in the same mortar prism. The variation in the results is still quite high; this could be caused by a different hardness in the interface region due to different chemical interactions. The elastic modulus of the mortar calculated from the results varies between 40 kN/mm^2 and 64 kN/mm^2.

Further and systematic investigations have to be done in order to obtain repeatability and to

define the error of measurement, in order for this measuring method to be applicable to different measuring problems.

Moisture- and temperature-induced deformations of a lightweight mortar

Furthermore, we measured the reactions of different building materials to external non-mechanical influences by means of embedded stiff microstrain sensors, especially temperature-induced deformation of mortars and moisture-influenced swelling of gypsum and lightweight mortar. For such purposes the choice of a low thermally sensitive and an almost non-swelling coating is very important. Otherwise, a moisture-induced swelling of the coating could feign a deformation of the matrix. Figure 30 illustrates the deformation of a lightweight mortar during heating/cooling and moistening cycles.

OUTLOOK

The excellent possibility of integrating optical fibers into structural components or into large sections of concrete structures opens the future for a built-in quality control of large structures. On the other hand, the deformation behavior of specially composed cementitious building materials could be better explored by means of integrated fiber sensors which do not react to the test object even if it is in the plastic stage.

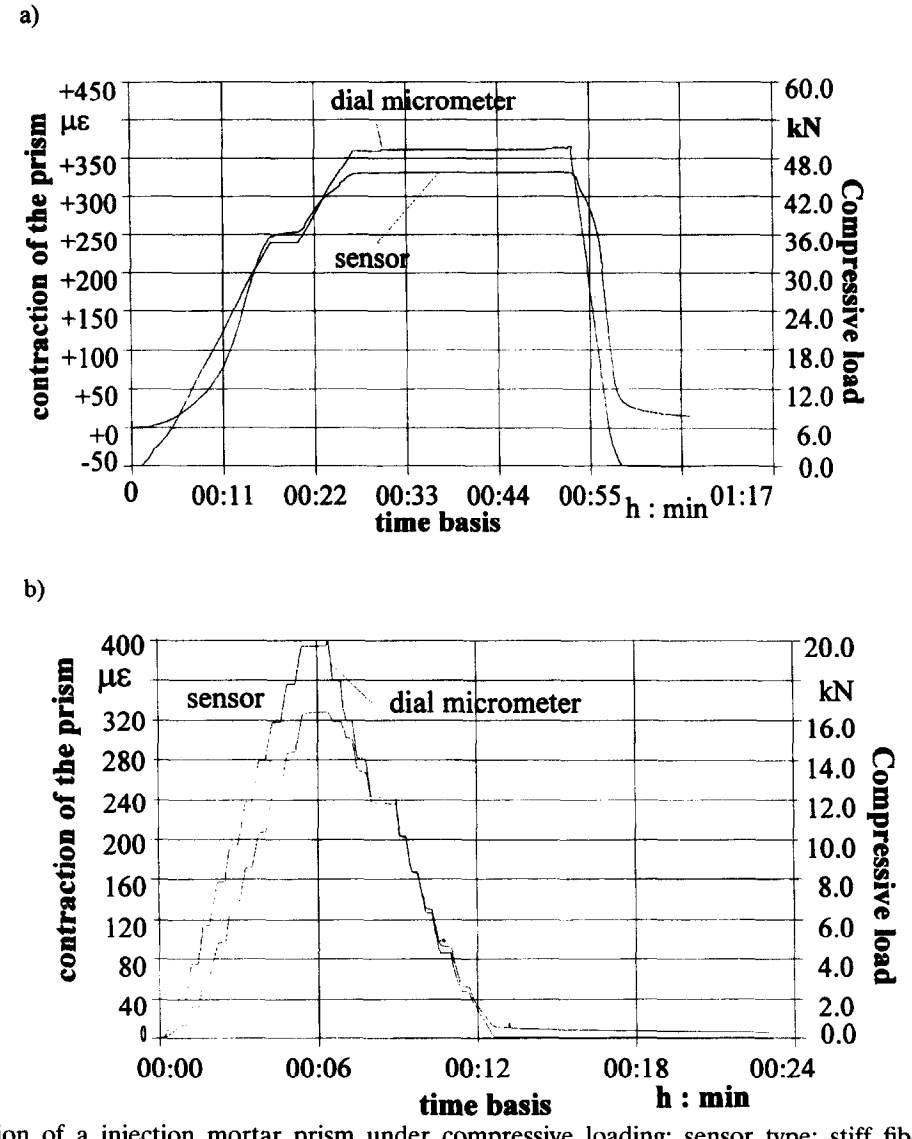

Fig. 28. Contraction of a injection mortar prism under compressive loading; sensor type: stiff fiber-optic microstrain sensors. (a) Coating: polymer, treated to obtain good bonding; sample age: 63 days. (b) Coating: inorganic material, untreated; sample age: 46 h.

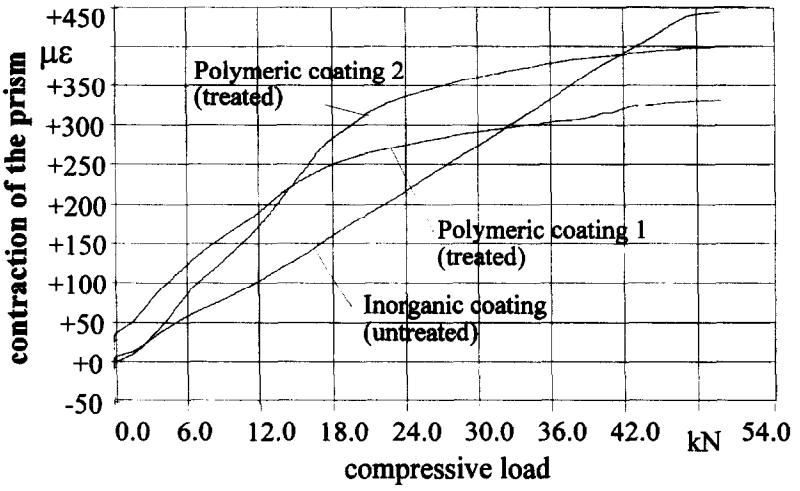

Fig. 29. Comparison of strain transfer in differently coated stiff micro optic sensors embedded in a fine-grained mortar (<2 mm), age: 63 days (polymeric coating: treated; inorganic coating: untreated).

Before optical fibers or sensors can be used as a reliable measuring method in direct contact with cementitious materials, and before they are accepted as established ones, a number of questions have to be solved in the future. The sensor manufacturer requires from the developer exact information about the design; the developers have to acquire a precise knowledge about the micromechanics in the sensing region, the long-term behavior of the materials and opto-electronic components used in the raw environment. They have to find an appropriate method of application that is also practicable under constructional conditions.

The knowledge gained in this field to date needs to be systematically deepened, and other newly developed micro optic sensors — i.e. Bragg grating fibers, very small fiber-optic moisture probes which will be able to deliver absolute values of moisture in building materials, or distributed moisture sensors — should be integrated into these investigations. Such a combination could be useful, on the one hand, for the evaluation of limits in sensor capability and on the other hand for a correlation of several influences, e.g. moisture and constraint, with the creep behavior of cement paste and mortar compositions.

SUMMARY AND CONCLUSIONS

It was demonstrated that the highly sensitive fiber-optic microstrain gages (Fabry–Pérot type) can be used without failure in the raw environment of structures. These sensors allow one to obtain more information about building reactions than ordinary strain gages or displacement meters, and they are unaffected by electromagnetic interference.

The paper describes the sensing technique, practical experience in application, demands on fiber sensors which are to be used for different applications to real structures, and contributes to the theoretical understanding of the design of sensors and interpretation of measurement results.

With such sensors a strain resolution between 0.06 $\mu\varepsilon$ and 0.1 $\mu\varepsilon$, depending on the different measuring instruments used, was achieved. The influence on strain due to transverse effects (pressure, bending) was estimated theoretically and simulated by simple test arrangements; its value was below the sensor's threshold of response. Temperatures have to be measured simultaneously and their influence on the strain behavior is automatically considered.

Two examples, involving the attachment of fiber sensors on the surfaces of the steel components of a structure, for solving typical measuring tasks in structural engineering have been described and evaluated:

application on the prestressed steels of a concrete highway bridge to measure its static and dynamic behavior during proof loading; and

application on the rebars of a concrete pile to assess its behavior under compressive loading.

The comparison of microstrain sensors with resistive strain gages (DMS) in laboratory revealed differences in measured strain. Lower strain values for DMS were observed in all measurements, both in the laboratory and on

site. The influence of the adhesive and method of attachment has to be determined in further investigations.

The known method of sensor attachment on steel rods was chosen in order to measure very small strain changes inside a newly built-up concrete wall during its hydration reaction and in connection with a cooling procedure. By means of short measuring probes fitted with fiber sensors and DMS and embedded in the reinforcing cage of the wall, strain deformations were detected with a resolution of 0.1 $\mu\varepsilon$. However, it is evident that this commonly used technique causes load concentrations at the measuring probe; the measuring environment is disturbed.

Directly embedded microstrain sensors without using stiff components avoid disturbance of the test object. Better results were obtained by using sensitive glass tubes designed with small 'ears' and surrounded with a thick protective layer. Otherwise, the load transmission was rather weak.

The best results were achieved by coating the sensor tubes with thin and well-bonding polymeric layers; examples of application for measurements of the deformation of cementitious mortar prisms caused by compressive loading or induced by moisture have been focused on. Good results were also achieved by using an inorganic coating (carbon layer). Before the tests were carried out as described, a number of optical fibers were investigated in order to find out the behavior of thin coatings in contact with cementitious materials; some results concerning the behavior of commonly used polymeric fiber coatings are presented.

In order to achieve strain values at very early ages of mortars, a new stress-free sensor arrangement developed by our group for embedment in hydraulically curing building materials was tested. It enabled, for the first time, the collection of measurement data about the material behavior in the interphase between rheology and solid state without disturbing the measuring environment. By way of example, the deformation behavior of injection mortar expanding admixtures during hardening in the first hours after casting, has been discussed.

All embedded sensors with thin coatings (layer thickness about 15–50 μm) survived the embedding procedure and remained functional for 8 or 11 months. It might be supposed that microstrain sensors with well-designed coatings withstand alkaline and mechanical attack during the hydration reaction and later; some theoretical aspects concerning the design of the sensors and the embedment procedure are discussed. Taking these criteria into account the long-term use of such microstrain sensors as structure-integrated measuring devices for on-line monitoring of structures or very early damage assessment will be possible.

ACKNOWLEDGEMENTS

The special sensor samples and the test facilities were arranged by Mr Basedau (Fiber Optics Group, IEMB). The SEM photographs were taken by Mr K. Wehner, the micro sections by Mrs Chr. Buwert, both of whom are staff of the Department of Building Chemistry, Building Material Analysis und Corrosion Prevention of the IEMB.

This work was supported by the BMBF of the Federal Republic of Germany, new Länder and the Berlin Senate Department of Science and Research (WIP program).

REFERENCES

1. Murphy, K. A. *et al.*, Extrinsic Fabry–Pérot optical fiber sensor. In *Proc. 8th Opt. Fib. Sens. Conf.*, Monterey, CA, January 1992. pp. 193–196.
2. Lenk, A., Dehnungsübertragung von Meßobjekten auf Dehnmeßstreifen. *Feingerätetechnik*, **24**(12) (1975) 535–536.
3. Onnen, O. & Fritz, H., Über die Bestimmung der mechanischen Spannungen bei Dehnungsmeßstreifen und ihren Einfluß auf die Meßgenauigkeit. *Feinwerktechnik*, **70**(10) (1969) 466–474.
4. Sirkis, J. S. & Haslach, H. W. Jr., Interferometric strain measurement by arbitrarily configured, surface-mounted, optical fibers. *J. Lightwave Technol.*, **8** (1990) 1497–1503.
5. Habel, W. & Hofmann, D., Determination of structural parameters concerning load capacity based on fiber Fabry–Pérot interferometers. In *Proc. European Conference on Smart Structures and Materials*, Glasgow, October 1994. SPIE vol. 2361, pp. 176–179.
6. Habel, W. & Holst, A., Vergleichende Verformungsmessungen an einem Stahlbetonpfahl mit Gleitmikrometer, DMS und Fasersensoren (Deformation measurements on a concrete pile by means of sliding micrometer, resistive strain gages and fiber optic sensors). In *Pfahlsymposium 1995*, TU Braunschweig, Institut für Grundbau, 23–24 February 1995.
7. Wolff, R. & Mießeler, H.-J., Neuartige Lichtwellenleitersensoren für die Überwachung von Felsbauwerken, Fels- und Erdankern und Gebirgsmeßstrecken (Novel optical fibre sensors for monitoring structures, rock and earth bolts and measured sections in rock). *Tunnel*, **5** (1992) 229–236.
8. Habel, W. & Hofmann, D., Strain measurements in reinforced concrete walls during the hydration reaction by means of embedded fibre interferometers. In

Proc. 2nd European Conference on Smart Structures and Materials, Glasgow, October 1994. SPIE Vol. 2361, pp. 180–183.
9. Habel, W. & Hillemeier, B., Results in monitoring and assessment of damages in large steel and concrete structures by means of fibre optic sensors. In *1995 North American Conference on Smart Structures and Materials*, San Diego, CA, February/March 1995. SPIE Vol. 2446, pp. 25–36.
10. Habel, W. & Polster, H., The influence of cementitious building materials on polymeric surfaces of embedded optical fibers for sensors. *J. Lightwave Technol.*, **13**(7) (1995) 1324–1330.
11. Mathews, C. T. & Sirkis, J. S., The interaction mechanics of interferometric optical fiber sensors embedded in a monolithic structure. In *Fiber Optic Smart Structures and Skins III*, SPIE Vol. 1370, 1990, pp. 142–153.
12. Pak, Y. E., Longitudinal shear transfer in fiber optic sensors. *Smart Mater. Struct.*, **1** (1992) 57–62.
13. Igarashi, S. & Kawamura, M., Effect of a size in bundled fibers on the interfacial zone between the fibers and the cement paste matrix. *Cement Concrete Res.*, **24**(4) (1994) 695–703.
14. Rohrbach, Chr., Spannungs- und Dehnungsmessungen an Beton. *Archiv für Technisches Messen*, **8246**(6) (July 1962, part 1) and **8246**(7) (August 1962, part 2).
15. Habel, W., Hofmann, D. & Basedau, F., Short-length fibre optic micro sensors for non-destructive assessment of the building materials and components behaviour. In *Proc. NDT-CE Symposium '95*, Berin, 26–28 October 1995. Part 1, pp. 583–596.